

## BRIEF REPORT

# Structurally abnormal collagen fibrils in abdominal aortic aneurysm resist platelet adhesion

Blain Jones<sup>1</sup>  | Anna Debski<sup>2</sup> | Chetan P. Hans<sup>3</sup> | Michael R. Go<sup>4</sup> | Gunjan Agarwal<sup>5</sup> 

<sup>1</sup>Biomedical Engineering Graduate Program, The Ohio State University, Columbus, Ohio, USA

<sup>2</sup>Department of Material Science and Engineering, The Ohio State University, Columbus, Ohio, USA

<sup>3</sup>Department of Cardiovascular Medicine, Dalton Cardiovascular Research Center, University of Missouri, Columbia, Missouri, USA

<sup>4</sup>Division of Vascular Surgery, The Ohio State University Wexner Medical Center, Columbus, Ohio, USA

<sup>5</sup>Department of Mechanical and Aerospace Engineering, The Ohio State University, Columbus, Ohio, USA

## Correspondence

Gunjan Agarwal, E503 Scott Laboratory, 201 W 19th Ave, Columbus, OH 43210, USA.

Email: agarwal.60@osu.edu

## Funding information

NIH Office of the Director, Grant/Award Number: 1S10OD025096-01A1; National Science Foundation, Grant/Award Number: 2000469; National Heart, Lung, and Blood Institute, Grant/Award Number: R01HL124155

## Abstract

**Background:** Platelet adhesion to the subendothelial collagen fibrils is one of the first steps in hemostasis. Understanding how structural perturbations in the collagen fibril affect platelet adhesion can provide novel insights into disruption of hemostasis in various diseases. We have recently identified the presence of abnormal collagen fibrils with compromised D-periodic banding in the extracellular matrix remodeling present in abdominal aortic aneurysms (AAA).

**Objective:** In this study, we employed multimodal microscopy approaches to characterize how collagen fibril structure impacts platelet adhesion in clinical AAA tissues.

**Methods:** Ultrastructural atomic force microscopy (AFM) analysis was performed on tissue sections after staining with fluorescently labeled collagen hybridizing peptide (CHP) to recognize degraded collagen. Second harmonic generation (SHG) microscopy was used on CHP-stained sections to identify regions of intact versus degraded collagen. Finally, platelet adhesion was identified via SHG and indirect immunofluorescence on the same tissue sections.

**Results:** Our results indicate that ultrastructural features characterizing collagen fibril abnormalities coincide with CHP staining. SHG signal was absent from CHP-positive regions. Additionally, platelet binding was primarily localized to regions with SHG signal. Abnormal collagen fibrils present in AAA (in SHG negative regions) were thus found to inhibit platelet adhesion compared to normal fibrils.

**Conclusions:** Our investigations reveal how the collagen fibril structure in the vessel wall can serve as another regulator of platelet–collagen adhesion. These results can be broadly applied to understand the role of collagen fibril structure in regulating thrombosis or bleeding disorders.

## KEYWORDS

abdominal aortic aneurysm, atomic force microscopy, blood platelets, collagen, fluorescence, microscopy

## 1 | INTRODUCTION

Collagen fibrils in the vessel wall not only provide tensile strength to the underlying tissue but also dictate cell–matrix interactions. Upon vascular injury, platelets adhere to the subendothelial collagen fibrils as the first step in the coagulation cascade. Platelet–collagen interaction is dependent on the accessibility of the binding sites of glycoprotein VI (GPVI)<sup>1</sup> and von Willebrand factor (VWF) on the collagen fibril.<sup>2–7</sup> A perturbation in the collagen fibril structure could thus impact platelet–collagen interaction and ensuing thrombus formation.<sup>8,9</sup> Vascular diseases such as abdominal aortic aneurysms (AAA) and atherosclerosis are characterized by significant, atypical remodeling of the vessel wall<sup>10,11</sup> and an imbalance in collagen synthesis and degradation.<sup>12,13</sup> However, little attention has been given to the thrombogenic potential of the remodeled, collagen-rich vessel wall, which initiates the coagulation cascade by modulating platelet adhesion to collagen fibrils.

We have recently identified the presence of abnormal collagen fibrils with compromised D-periodic banding in the remodeled regions of AAA,<sup>14</sup> by using ultrastructural atomic force microscopy (AFM) and transmission electron microscopy (TEM). However, the functional consequences of these abnormal fibrils remain to be investigated. In this study, we employed multimodal microscopy approaches to understand how the collagen fibril structure affects platelet adhesion in clinical AAA tissue. To identify abnormal collagen via histochemical staining, AFM analysis was performed on tissue sections stained with collagen hybridizing peptide (CHP), a reagent that recognizes degraded collagen.<sup>15–17</sup> Second harmonic generation (SHG) microscopy (which recognizes intact collagen) was used on CHP-stained sections to identify regions of normal versus abnormal collagen. Finally, platelet adhesion was identified via SHG and indirect immunofluorescence on the same sections. Our results indicate how platelet adhesion in AAA is localized to regions with normal fibrils. These insights can be used to better understand the hemostatic mechanisms involved in the pathogenesis of AAA and other diseases.

## 2 | MATERIALS AND METHODS

### 2.1 | Aortic tissue

Human AAA tissue was obtained in accordance with an approved institutional review board (IRB) protocol from The Ohio State University.<sup>14</sup> A ~3 x 3 cm segment of anterior aortic sac was excised from patients who were undergoing elective open aneurysm repair. Tissues were obtained from ( $n = 3$ ) non-Hispanic White male patients (ages 65–75 years). Non-aneurysmal control samples ( $n = 3$ ) were from the infrarenal segment of aorta obtained from autopsies within 24 h of death, in accordance with an approved IRB protocol from Wayne State University.<sup>18</sup> Murine aortic tissue was obtained from saline (control) or angiotensin-II (AAA model) infused animals via approved animal-use protocols as described in our previous study.<sup>14</sup>

### Essentials

- Platelet adhesion to collagen is dependent on the collagen fibril structure.
- Remodeling of the vessel wall in abdominal aortic aneurysms (AAA) consists of abnormal collagen fibrils with compromised structure.
- Multimodal microscopic analysis could discern regions of normal and abnormal collagen fibrils in AAA tissue sections.
- Native collagen fibrils facilitate platelet binding, while abnormal collagen in AAA was resistant to platelet binding.

### 2.2 | Collagen hybridizing peptide staining

Aortic tissues were fixed with 4% paraformaldehyde, embedded in optimal cutting temperature (OCT) compound, flash frozen in liquid nitrogen, and stored at  $-80^{\circ}\text{C}$ . For CHP staining, a solution of 1  $\mu\text{M}$  Cy3-conjugated CHP (3Helix) in phosphate buffered saline (PBS) was heated at  $80^{\circ}\text{C}$  for 5 min followed by quenching on ice cold water and centrifugation. Cryosections (5  $\mu\text{m}$ ) of aortic tissue were mounted onto glass slides, washed with PBS, and incubated with CHP solution overnight at  $4^{\circ}\text{C}$ . Thereafter, the samples were washed and either mounted and cover-slipped for fluorescence microscopy or air dried and left unmounted for AFM analysis.

### 2.3 | Second harmonic generation microscopy

Imaging was performed using a 25x water immersion objective lens on an Olympus FV1000 MPE Multiphoton Laser Scanning Confocal Microscope equipped with a Mai Tai DeepSee titanium-sapphire laser. Two-photon imaging of forward scattered light was utilized for SHG of collagen with an excitation wavelength of 950 nm. Single-photon images were acquired from the very same regions to detect CHP or immunofluorescence signal via a tetramethyl rhodamine (TRITC) filter. Olympus FluoView software was used to control the laser scanning and image acquisition at fixed exposure times.

### 2.4 | Atomic force microscopy

CHP-stained sections were imaged using a Bruker Resolve AFM coupled to a Zeiss Observer light microscope. AFM images (10 x 10  $\mu\text{m}$ , 1024 x 1024 pixels) were acquired in ambient air from selected (at least  $n = 3$ ) CHP-positive (or -negative) regions in each fluorescence image using the MiroView feature in ScanAsyst mode. The AFM height and error images were used to identify normal versus abnormal collagen fibrils based on the contrast and depth of their D-periods as shown earlier.<sup>14</sup>

## 2.5 | Platelet adhesion assay

Whole blood (~10 ml) was obtained from male or female healthy adults (aged 18–50 years) in 3.2% sodium citrate tubes via venipuncture in accordance with our IRB protocol (#2011H0365). Human platelet-rich plasma (PRP) was isolated from whole blood by centrifugation at 200 g for 10 min and used within 30 min. Platelet-poor plasma (PPP) was extracted by centrifugation of PRP at 1000 g for 10 min. Cryosections of aortic tissue were washed in PBS, blocked with 2% bovine serum albumin (BSA), and incubated with 10% PRP (diluted in PPP) at room temperature for 30 min under static conditions. Sections were then washed to remove unbound platelets, blocked with 2% BSA, and incubated with primary anti-GP1b antibody (1:1000) followed by Alexa Fluor 568 conjugated secondary antibody (1:2500). After final washes, the sections were mounted and imaged for collagen (SHG) and platelet adhesion (indirect immunofluorescence) signal. Experiments were repeated with whole blood from  $n = 3$  donors and results were compared across ( $n = 3$ ) AAA and control tissues for each matched blood donor.

## 2.6 | Image analysis

ImageJ (National Institutes of Health) was used to ascertain areal fraction of degraded (CHP) to total collagen (SHG + CHP) signal in

multiphoton images by analyzing  $n = 3$  images per sample. The extent of platelet adhesion in AAA and control tissues was ascertained by comparison of areal fraction of indirect immunofluorescence with SHG signal in ( $n = 3$ ) 50  $\mu\text{m}$  diameter regions of interest (ROIs) in fluorescence images from each sample. For AAA tissues, platelet adhesion was also compared in ROIs from SHG-positive versus SHG-negative regions.

Statistically significant differences for the two group comparisons were determined using a two-sided t-test (SAS JMP software, version 14.0). A  $P$ -value  $< .05$  was considered significant.

## 3 | RESULTS AND DISCUSSION

To detect degraded collagen, we employed histochemical staining of aortic sections with Cy3-conjugated CHP. As shown in Figure 1A, control sections of human aortic tissue displayed a low level of CHP staining in the medial layer and even lower staining in the adventitia. Clinical AAA sections (Figure 1B), on the other hand, exhibited an overall higher CHP fluorescence with a number of high intensity “hot spots” in the remodeled tissue. Unstained tissues (insets) exhibited negligible auto-fluorescence at this excitation wavelength. A similar observation was made in murine models of AAA in which CHP signal was detected in the remodeled regions of abdominal aorta of angiotensin-II induced mice but not in that of saline-infused controls

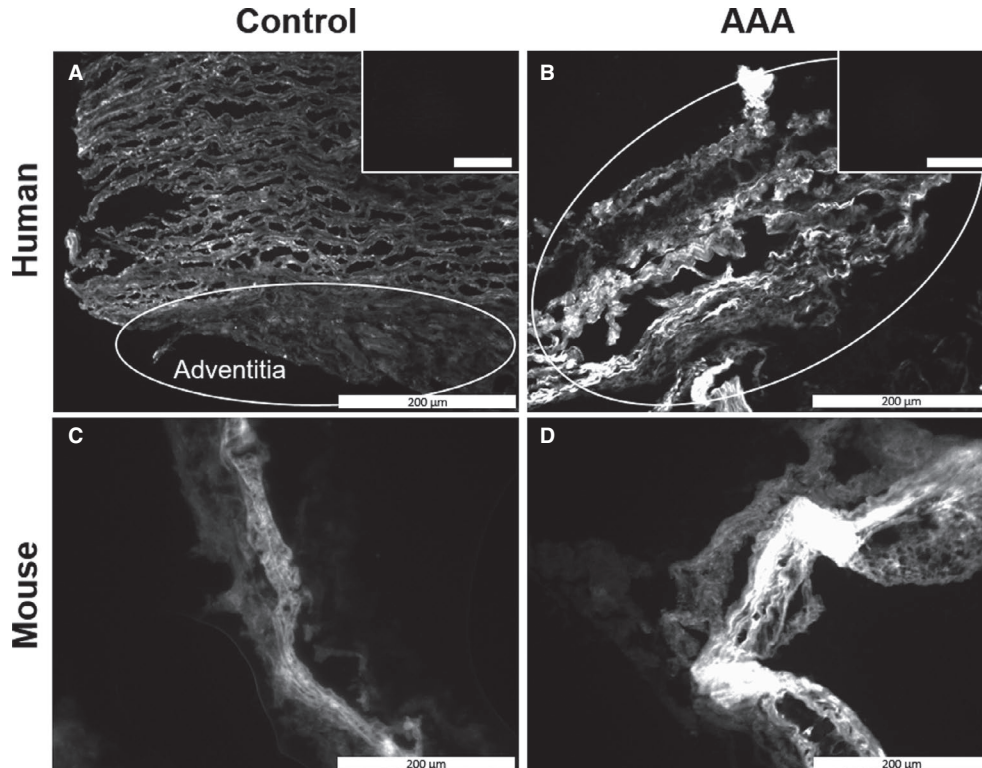


**FIGURE 1** Wide-field fluorescence microscopy of control (A, C) and abdominal aortic aneurysms (AAA; B, D) tissues with collagen hybridizing peptide (CHP) staining as indicated. Only weak CHP staining in the adventitial region of both human and murine control aortas was observed. Unstained tissues had negligible fluorescence (insets in A and B). The remodeled regions in AAA tissues showed strong CHP staining indicating presence of degraded collagen. All images were taken at 20x magnification

(Figure 1C,D). CHP is reported to recognize damaged collagen generated *in vitro*<sup>17,19</sup> and present in human diseases such as osteoarthritis,<sup>15</sup> liver fibrosis,<sup>20</sup> and intervertebral disc degeneration.<sup>21</sup> We show here how damaged collagen is also present in vascular diseases such as AAA.

Little is understood about the ultrastructure of damaged collagen fibrils. To characterize the collagen fibril ultrastructure in regions with/out CHP staining, we utilized AFM, an ultrastructural microscopy technique. As shown in Figure 2, AFM images were acquired from CHP-negative or CHP-positive regions identified in

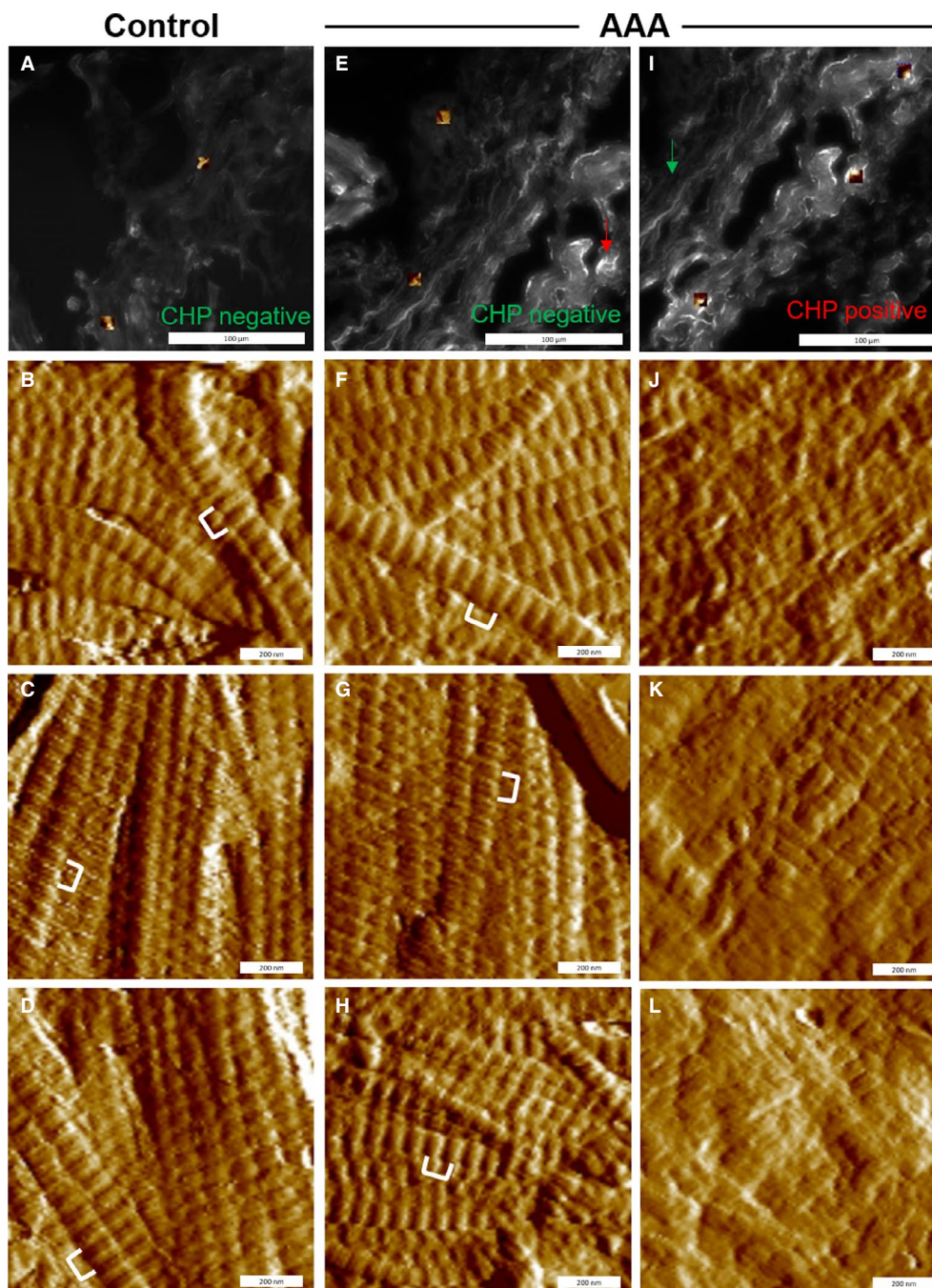


**FIGURE 2** Integrated fluorescence and atomic force microscopy (AFM) analysis of collagen hybridizing peptide (CHP)-stained tissues. AFM images were acquired from regions negative (A–H) or positive (I–L) for strong CHP staining in control or clinical abdominal aortic aneurysms (AAA) tissues as indicated. Small colored boxes in (A), (E), and (I) denote the location of AFM images in panels (B–D), (F–H), and (J–L), respectively. In CHP-negative regions from control aorta or AAA, normal collagen fibrils with distinct D-periodicity (white brackets in B and F) were observed. D-periodicity refers to the uniform (~66 nm) periodic banding pattern along collagen fibrils, which arises due to the gap-overlap zones generated when collagen molecules assemble to form a fibril. CHP-positive regions in AAA consisted of abnormal collagen fibrils with diminished D-periodicity (J–L). Arrows in (E) and (I) show location of CHP positive region in CHP negative image or vice versa

fluorescence microscopy images. CHP-negative regions in control tissue (Figure 2A-D) and in AAA (Figure 2E-H) were either completely devoid of collagen fibrils (i.e., consisted of ground material)

or exhibited fibrils that were normal in structure. In contrast, AFM images from CHP-positive regions in AAA tissue revealed an abundance of abnormal collagen fibrils (with diminished contrast

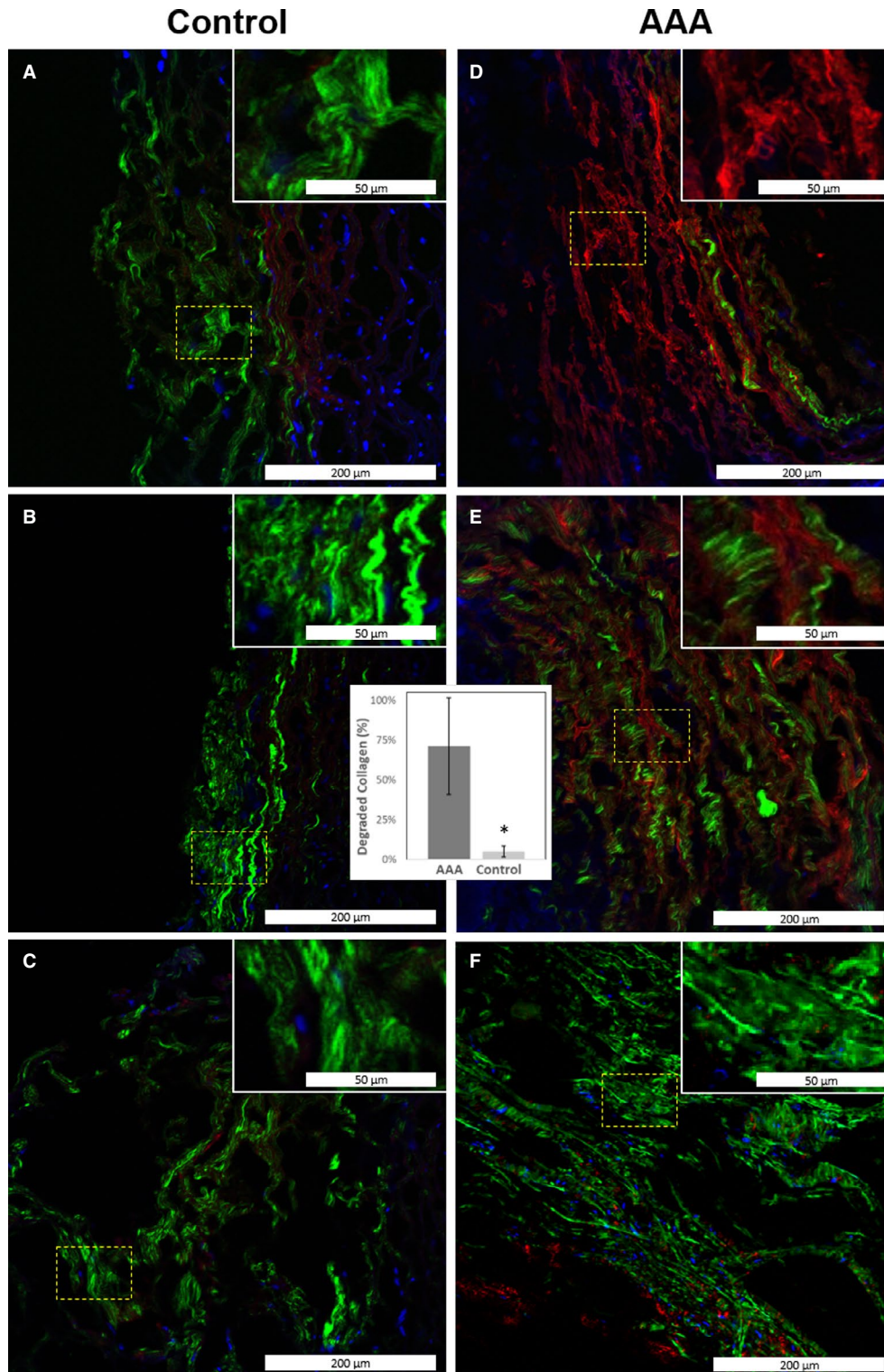


**FIGURE 3** Multiphoton images of control aorta (A–C) and clinical abdominal aortic aneurysms (AAA; D–F) showing localization of normal (green: second harmonic generation [SHG]) and degraded collagen (red: collagen hybridizing peptide [CHP]). Blue: DAPI stain showing cell nuclei. While the control samples only exhibited SHG signal, the remodeled regions in AAA showed both CHP staining and SHG signal in spatially distinct regions. Inset: areal fraction of degraded collagen (CHP) to total collagen (CHP+SHG) was significantly greater in AAA ( $71.2\% \pm 30.2\%$ ) than in controls ( $5.24\% \pm 3.4\%$ ;  $P < .05$ ). All images taken at 25x magnification

in D-periodicity) along with the presence of few normal fibrils (Figure 2I-L). We thus elucidate that ultrastructural abnormalities in collagen fibril coincide with CHP-positive regions in AAA. Our results are consistent with a previous study in which TEM imaging was used to elucidate how immunogold-labeled CHP localized to collagen fibrils that exhibited a diminished contrast in D-periodicity.<sup>17</sup>

To localize regions of normal and abnormal collagen in a high-throughput manner compatible with routine histology, we employed another multimodal approach: SHG microscopy along with single-photon fluorescence on CHP-stained samples. Native, intact collagen fibrils generate a strong SHG signal while collagen malformation<sup>22</sup> can result in a lower SHG signal. As shown in Figure 3A-C, abundant SHG but negligible CHP signal was observed in the adventitia of control tissues. On the other hand, in AAA tissue both SHG

and CHP signals were heterogeneously distributed (Figure 3D-F). Some areas comprised primarily of CHP signal, while others were devoid of CHP but had strong SHG signal. Regions with SHG signal interspersing CHP staining were also found in AAA. Little to no co-localization between the CHP and SHG signals was observed in our study, consistent with previous studies;<sup>15,19</sup> that is, SHG-positive regions were CHP negative and vice versa. Of the total collagen, the percent of degraded collagen (inset of Figure 3) was estimated to be significantly greater in AAA ( $71.2\% \pm 30.2\%$ ) than that of control tissue ( $5.24\% \pm 3.4\%$ ,  $P < .05$ ).

Finally, we evaluated how platelet adhesion to collagen was affected by the presence of normal versus abnormal fibrils, by employing multimodal SHG and indirect immunofluorescence. As shown in Figure 4A-D, control tissues showed platelet binding primarily to the

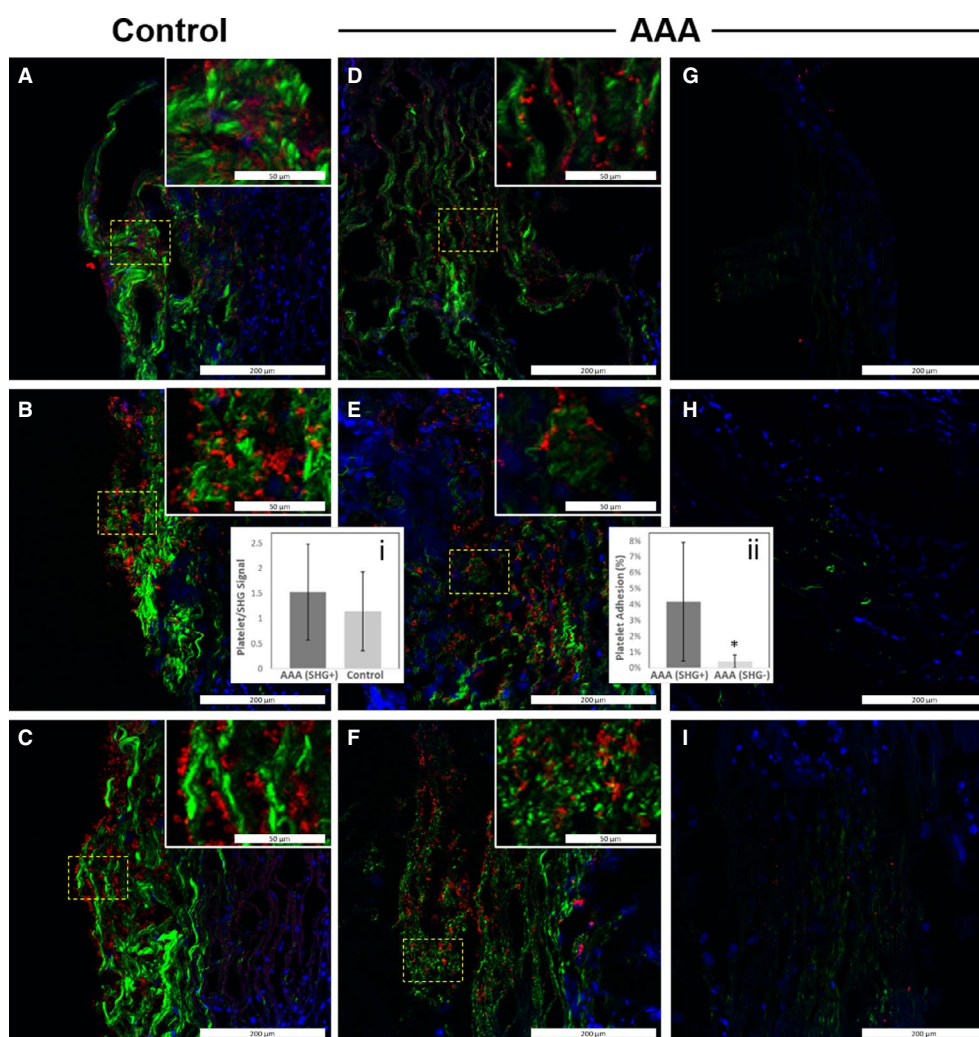


**FIGURE 4** Multiphoton images of control aorta (A-C) clinical abdominal aortic aneurysms (AAA; D-I) showing localization of platelet binding. Representative images obtained using blood from three different donors are shown. Red: immunofluorescence (bound platelets); green: second harmonic generation (SHG) signal (normal collagen); blue: DAPI stain (cell nuclei). Platelet binding to SHG-rich regions occurred in both control aorta (A-C) and AAA tissue (D-F). Inset i: areal fraction of platelet signal for SHG-rich regions with fixed regions of interest (ROIs). No significant difference in extent of platelet adhesion was obtained between AAA ( $1.53 \pm 0.95$ ) and control tissue ( $1.14 \pm 0.78$ ;  $P > .05$ ). In AAA tissue, platelet binding was minimal in regions that were poor in SHG signal (G-I). Inset ii: areal fraction of platelet adhesion in SHG-rich versus SHG-poor regions with fixed ROIs. Significantly higher platelet adhesion was obtained in SHG-rich regions ( $4.2\% \pm 3.7\%$ ) compared to SHG-poor regions ( $0.41\% \pm 0.38\%$ ;  $P < .05$ ). All images were taken at 25x magnification

adventitial collagen, which also exhibited strong SHG signal. In AAA tissues, platelets also localized to regions showing strong SHG signal (Figure 4D–F) and were nearly absent in regions devoid of SHG signal (Figure 4G–I). We noted that the platelet and SHG signals did not entirely overlap (assessed by Pearson's coefficient). This could be because the presence of platelets (~2  $\mu\text{m}$ ) interfered with SHG signal arising from the very same site on the collagen fibril. Earlier studies have encountered a similar feature when using SHG in combination with indirect immunofluorescence to detect collagen.<sup>23</sup> We performed image analysis to compare the areal ratio of platelet adhesion to regions with/out SHG signal. For SHG-positive regions (Figure 4, inset i) no statistically significant difference was observed between AAA and controls ( $P > .05$ ). However, in AAA tissues, platelet binding was significantly higher for regions with strong SHG signal compared to regions devoid of SHG signal ( $P < .05$ , Figure 4, inset ii).

Taken together, our results thus show that platelet adhesion in AAA tissue is primarily localized to regions consisting of normal collagen fibrils and is resistant to regions with abnormal collagen fibrils. These insights can help explain the heterogeneity in the reactivity of platelets to various collagen-enriched regions as reported for atherosclerotic plaques in a previous study.<sup>24</sup> Currently, assessment of coagulopathy in endovascular or open surgical repair in AAA is done via platelet function and hemostatic indicators in the plasma. In one report, diminished platelet adhesiveness in AAA remained abnormal even after transfusion of normal blood.<sup>25</sup> Our results indicate that thrombogenicity of the vessel wall (i.e., presence of abnormal collagen) could be another important determinant of coagulopathy. Along these lines, insertion of collagen-impregnated grafts could reduce blood loss in patients undergoing infrarenal aortic reconstruction.<sup>26</sup>

Intraluminal thrombus (ILT) resulting from damage to the endothelium in the initial stages of AAA is reported in more than 75% of clinical AAA. ILT is understood to play a protective role in the early stages of aneurysm formation<sup>27</sup> and non-occlusive ILT correlates with reduced peak wall stress<sup>28</sup> and may lower its rupture potential.<sup>29</sup> The use of anti-thrombotic therapies in AAA thus continues to be a matter of debate. It should be noted that our study employed AAA tissue from an advanced stage of the disease characterized by extensive remodeling. The collagen fibril structure is likely to be normal and pro-thrombogenic in the early (compared to advanced) stage of the disease. Assessment of collagen quality and thrombogenicity of the vessel wall at various stages of the growing AAA may provide novel insight into hemostatic mechanisms linked to the pathogenesis of this disease. A limitation of our study was that we only examined platelet adhesion under static conditions. Our results are still relevant as the rapid first phase of platelet–collagen adhesion occurs within a minute under both static and flow conditions.<sup>30</sup> Future studies, using a flow chamber to mimic arterial shear rates, would provide a more comprehensive evaluation of downstream processes like platelet aggregation and thrombus formation.

#### ACKNOWLEDGMENTS

This work was supported by the NSF award 2000469, NIH 1S10OD025096-01A1, and NIH grant R01HL124155 (CPH).

#### CONFLICTS OF INTEREST

None of the authors have any real or potential conflicts of interest with this work.

#### AUTHOR CONTRIBUTIONS

BJ performed all experiments, analyzed data, and wrote the manuscript. AD optimized the SHG and CHP staining protocols. CH and MG provided aortic tissue from healthy donors and AAA patients, respectively. GA designed the research and provided funding and resources for the proposed work. All authors reviewed and edited the manuscript.

#### ORCID

Blain Jones  <https://orcid.org/0000-0002-8994-3069>

Gunjan Agarwal  <https://orcid.org/0000-0003-3731-2107>

#### REFERENCES

1. Agarwal G, Smith AW, Jones B. Discoidin domain receptors: Micro insights into macro assemblies. *Biochim Biophys Acta - Mol Cell Res.* 2019;1866(11):118496. 10.1016/j.bbamcr.2019.06.010
2. Muggli R, Baumgartner HR. Collagen induced platelet aggregation: Requirement for tropocollagen multimers. *Thromb Res.* 1973;3(6):715-728. 10.1016/0049-3848(73)90018-2
3. Brass LF, Bensusan HB. The role of collagen quaternary structure in the platelet: collagen interaction. *J Clin Invest.* 1974;54(6):1480-1487. 10.1172/JCI107896
4. Jaffe R, Deykin D. Evidence for a structural requirement for the aggregation of platelets by collagen. *J Clin Invest.* 1974;53(3):875-883. 10.1172/JCI107628
5. Simons ER, Chesney CMI, Colman RW, Harper E, Samberg E. The effect of the conformation of collagen on its ability to aggregate platelets. *Thromb Res.* 1975;7(1):123-139. 10.1016/0049-3848(75)90130-9
6. Sylvester MF, Yannas IV, Salzman EW, Forbes MJ. Collagen banded fibril structure and the collagen-platelet reaction. *Thromb Res.* 1989;55(1):135-148. 10.1016/0049-3848(89)90463-5
7. Butler LM, Metson-Scott T, Felix J, et al. Sequential adhesion of platelets and leukocytes from flowing whole blood onto a collagen-coated surface: requirement for a GpVI-binding site in collagen. *Thromb Haemost.* 2007;97(5):814-821. 10.1160/TH06-08-0439
8. Adili F, Balzer JO, Ritter RG, et al. Ruptured abdominal aortic aneurysm with aorto-caval fistula. *J Vasc Surg.* 2004;40(3):582. 10.1016/S0741-5214(03)00921-2
9. Michel JB, Martin-Ventura JL, Egido J, et al. Novel aspects of the pathogenesis of aneurysms of the abdominal aorta in humans. *Cardiovasc Res.* 2011;90(1):18-27. 10.1093/cvr/cvq337
10. Zamaneh Kassiri RB. Extracellular matrix remodelling and abdominal aortic aneurysm. *J Clin Exp Cardiol.* 2013;04(08):1-8. 10.4172/2155-9880.1000259
11. Lindeman JHNN, Ashcroft BA, Beenakker JWM, et al. Distinct defects in collagen microarchitecture underlie vessel-wall failure in advanced abdominal aneurysms and aneurysms in Marfan syndrome. *Proc Natl Acad Sci USA.* 2010;107(2):862-865. 10.1073/pnas.0910312107
12. Dobrin PB, Mrkvicka R. Failure of elastin or collagen as possible critical connective tissue alterations underlying aneurysmal dilatation. *Vascular.* 1994;2(4):484-488. 10.1177/096721099400200412
13. Thompson RW, Geraghty PJ, Lee JK. Abdominal aortic aneurysms: basic mechanisms and clinical implications. *Curr Probl Surg.* 2002;39(2):110-230. 10.1067/msg.2002.121421

14. Jones B, Tonniges JR, Debski A, et al. Collagen fibril abnormalities in human and mice abdominal aortic aneurysm. *Acta Biomater.* 2020;110:129-140. 10.1016/j.actbio.2020.04.022
15. Hwang J, Huang Y, Burwell TJ, et al. In situ imaging of tissue remodeling with collagen hybridizing peptides. *ACS Nano.* 2017;11(10):9825-9835. 10.1021/acsnano.7b03150
16. Bennink LL, Li Y, Kim B, et al. Visualizing collagen proteolysis by peptide hybridization: From 3D cell culture to in vivo imaging. *Biomaterials.* 2018;183:67-76. 10.1016/J.BIOMATERIALS.2018.08.039
17. Zitnay JL, Li Y, Qin Z, et al. Molecular level detection and localization of mechanical damage in collagen enabled by collagen hybridizing peptides. *Nat Commun.* 2017;8: 10.1038/ncomms14913
18. Cheng J, Koenig SN, Kuivaniemi HS, Garg V, Hans CP. Pharmacological inhibitor of notch signaling stabilizes the progression of small abdominal aortic aneurysm in a mouse model. *J Am Heart Assoc.* 2014;3(6):e001064. 10.1161/JAHA.114.001064
19. Kaa K, Haasterecht L, Elgersma A, et al. Effective enzymatic debridement of burn wounds depends on the denaturation status of collagen. *Wound Repair Regen.* 2020;28(5):666-675. 10.1111/WRR.12827
20. Jaramillo C, Guthery SL, Lowichik A, et al. Quantitative liver fibrosis using collagen hybridizing peptide to predict native liver survival in biliary atresia: a pilot study. *J Pediatr Gastroenterol Nutr.* 2020;70(1):87-92. 10.1097/MPG.0000000000002505
21. Xiao L, Majumdar R, Dai J, et al. Molecular detection and assessment of intervertebral disc degeneration via a collagen hybridizing peptide. *ACS Biomater Sci Eng.* 2019;5(4):1661. 10.1021/ACSBIOMATERIALS.9B00070
22. Williams RM, Zipfel WR, Webb WW. Interpreting second-harmonic generation images of collagen I fibrils. *Biophys J.* 2005;88(2):1377-1386. 10.1529/biophysj.104.047308
23. Theodossiou TA, Thrasivoulou C, Ekwobi C, Becker DL. Second harmonic generation confocal microscopy of collagen type I from rat tendon cryosections. *Biophys J.* 2006;91(12):4665. 10.1529/BIOPHYSJ.106.093740
24. van Zanten GH, de Graaf S, Slootweg PJ, et al. Increased platelet deposition on atherosclerotic coronary arteries. *J Clin Invest.* 1994;93(2):615. 10.1172/JCI117014
25. Ls F, Ne M, Rb D. Platelet dysfunction associated with abdominal aortic aneurysm. *Am J Clin Pathol.* 1980;74(5):701-705. 10.1093/AJCP/74.5.701
26. Barral X, Gay JL, Favre JP, Gournier JP. Do collagen-impregnated knitted Dacron grafts reduce the need for transfusion in infrarenal aortic reconstruction? *Ann Vasc Surg.* 1995;9(4):339-343. 10.1007/BF02139404
27. Cameron SJ, Russell HM, Phillip OA. Antithrombotic therapy in abdominal aortic aneurysm: Beneficial or detrimental? *Blood.* 2018;132(25):2619-2628. 10.1182/blood-2017-08-743237
28. Martufi G, Lindquist Liljeqvist M, Sakalihan N, et al. Local diameter, wall stress, and thrombus thickness influence the local growth of abdominal aortic aneurysms. *J Endovasc Ther.* 2016;23(6):957-966. 10.1177/1526602816657086
29. Horvat N, Virag L, Karšaj I. Mechanical role of intraluminal thrombus in aneurysm growth: a computational study. *Biomech Model Mechanobiol.* 2021;20(5):1819-1832. 10.1007/S10237-021-01478-W
30. Reiningger AJ, Bernlochner I, Penz SM, et al. A 2-step mechanism of arterial thrombus formation induced by human atherosclerotic plaques. *J Am Coll Cardiol.* 2010;55(11):1147-1158. 10.1016/J.JACC.2009.11.051

**How to cite this article:** Jones B, Debski A, Hans CP, Go MR, Agarwal G. Structurally abnormal collagen fibrils in abdominal aortic aneurysm resist platelet adhesion. *J Thromb Haemost.* 2022;20:470–477. doi:[10.1111/jth.15576](https://doi.org/10.1111/jth.15576)